COFFERDAM (ÇOKAL DAM-TURKEY) BREACH INUNDATION MODELLING USING LISFLOOD-FP

Assist. Prof. Dr. Hasan ÖZDEMİR

COFFERDAM (ÇOKAL DAM-TURKEY) BREACH INUNDATION MODELLING USING LISFLOOD-FP

Assist. Prof. Dr. Hasan ÖZDEMİR[1]

The Cofferdam failure occurred on November 16, 2007, releasing 12,307,513 m^3 of water. All agricultural land and farm houses on the Kavak Plain were inundated as a result of this failure, but no human lives were lost. This paper describes the results of an inertial and a Roe formulation implemented within the LISFLOOD-FP hydraulic model using different boundary conditions produced by MacDonald and Langridge-Monopolis (1984), Froehlich (1995 a,b) and Chinnarasri et al. (2004) regression equation-based breach flow prediction methods and using 10m resolution DEM data. The modelling results were evaluated against flood depth, inundation area, arrival times and fit statistics using a real flood extent map. The results show that MacDonald and Langridge-Monopolis (1984) breach flow prediction is shown to give better results in both the inertial and Roe models, with a peak breach flow of 3016.15m^3s^{-1} and total 2.67 hours inflow. In addition, MacDonald and Langridge-Monopolis using the Roe model gave the best fit (79.8%) with the real flood extent map. However, the Roe model has higher mass error than the inertial model. It is suggested that the use of extra detail DEM resolution and discharge data of the tributaries joining the Kavak River below the Dam location will be advantageous for modelling and risk management of a probable future Çokal Dam breach inundation.

Flooding is one of the most devastating hazards in the world. Based on EM-DAT data, more than 4 million people were killed in the world as a result of general flood events between 1900 and 2011, and their damage reached $338 billion (EM-DAT 2011). Floods can be caused by natural factors (e.g. intensive rainfall, physical and morphometric characteristics of river channel and basin etc.) and man-made factors (e.g. some engineering misapplications on the river channels, sewer systems, embankments, dams etc.). The consequences of these man-made floods can be more catastrophic than the natural floods. Especially those of dams,

1] *Physical Geography Division, Geography Department, Istanbul University, 34459, Turkey. Tel: +90 212 455 5700 E-mail: ozdemirh@istanbul.edu.tr*

which are structures that form a "barrier" that obstructs the river and its flow, are built for many purposes such as flood control, irrigation, hydropower generation, water supply etc. However, the failure of a dam caused by earthquakes, differential settlement, seepage, overtopping, dam structure deterioration, rockslide, poor construction and sabotage (Rico et al. 2008a; Rico et al. 2008b) produces a very large amount of water, creates more damages than normal river floods and could lead to tremendous loss of lives and assets in downstream areas (Hsu et al. 2000; Chang et al. 2000; Chen et al. 2005).

There are many examples of dam failures and their consequences from all around the world (BSMH 2004; Froehlich 2008; Warren 2011). To be able to estimate potential losses more accurately in close proximity to the dam, breach parameters of the dam/embankment must be chosen very sensitively in breach-inundation modelling. Generally, modelling of dam breaching failure requires solving two problems - determining the outflow from the breach and routing the computed flood wave through the downstream flood plain (Chinnarasri et al. 2004). To estimate the peak discharge and flood hydrograph through the breach, some researchers such as Kirkpatrick (1977), SCS (1981), Hagen (1982), Sing and Snorrason (1984), MacDonald and Langridge-Monopolis (1984), Costa (1985), Evans (1986), Von Thun and Gillette (1990), Froehlich (1995 a,b) and Chinnarasri et al. (2004) used regression relations between the observed peak outflow and reservoir volume, depth of water, dam height or some combination thereof, whilst others such as Fread (1988), Singh and Scarlatos (1989) and Tingsanchali and Chinnarasri (2001) used numerical simulation based on the breach formation model to estimate the peak discharge. Breach size and time depend on type and geometry of the dam, topography of the foundation and surrounding area, properties of the materials making up the dam, and reservoir head and volume at the time of failure. Defining breach parameters for dam break studies, therefore, is a process that necessitates combining information from available empirical relationships, historical experience and the exercise of professional judgment.

NWS-DAMBRK (Fread 1988), NWS-FLDWAV (Fread 2000) and the HEC-RAS model (HEC 2010) from the U.S. Army Corps of Engineers were most commonly used for performing dam breach outflow hydrograph computation and downstream routing. All these models work with one-dimensional computational flow models. In reality, the hydrodynamics induced by a dam break are complex and three-dimensional (De Maio et al. 2004; Nagata et al. 2005; Mohammadi 2008). However, In comparison with the 3D equations, the cross-section-averaged (1D shallow water equations) or depth averaged (2D shallow water equations) mathematical formulations require less computational cost and thus become

the main framework of dam break flow computation, even though the shallow water equations are based on some assumptions (Toro 2001). For this type of problem, finite volume Godunov-type models have become a standard tool in computational hydraulics due to their inherent shock-capturing capability and conservative properties (Toro and Garcia-Navarro 2007; Wang et al. 2011).

LISFLOOD-FP is a software package designed to model the propagation of water over complex topography typically represented by raster data. It is originally derived from 1D shallow water theory for use in 2D storage cell inundation models where flows in x and y cartesian directions are decoupled. The package is a mature system that has undergone extensive development and testing since conception (e.g. Bates and De Roo 2000; Hunter et al. 2005; Bates et al. 2010). LISFLOOD-FP consists of a collection of numerical schemes implemented to solve a variety of mathematical approximations of the 2D shallow water equations of different complexity (ranging from an extremely simple diffusive model to a shock capturing Godunov-type scheme based on the Roe Riemann solver). Neal et al. (in press) tested different LISFLOOD-FP codes such as inertial wave (ACC), diffusion wave (ATS) and Roe (ROE) in a hypothetical dam break. They found that LISFLOOD-ROE, which is based on the Godunov approach and uses an approximate Riemann solver by Roe (Roe 1981), provided a similar solution to the industry shallow water models, whilst LISFLOOD-ACC was the least accurate and had a 30% volume error and LISFLOOD-ATS provided inaccurate solution due to lack of shock capturing capability in the test case. However, they suggested that LISFLOOD-ACC was usually the quickest model, which would be particularly advantageous for real-time inundation forecasting, Monte Carlo type analysis or large model applications.

The aim of this study is the modelling and calibration of cofferdam breach inundation through the Kavak River plain using different LISFLOOD-FP models and different breach hydrographs according to MacDonald and Langridge-Monopolis (1984), Froehlich (1995 a, b) and Chinnarasri et al. (2004). Firstly the site and the event are described, secondly the data used, hydraulic model and its application procedures are set out under the data and methods. Finally, the results are presented and discussed in terms of arrival times, flood extents and flood depths overall modelling and the real event before the conclusions are drawn and implications stated.

Site and event description

Çokal Dam is located on the Kavak River in between Tekirdağ and Çanakkale district in Thrace Peninsula, Turkey. The basin lies between latitudes 40°34' to 40°54' N and longitudes 26°50' to 27°19' E, its elevation changes between 0-920m above sea level and drains an area of 773 km^2 (Fig. 1). The basin is predominantly formed by Eocene formation comprising fine – to medium - grained sandstone, yellowish – grey laminated claystone with intercalations of tuff, fine-grained turbiditic sandstone and mudstone (Sümengen and Terlemez 1991). Ganos fault (GF) which is an active dextral strike-slip fault and major branch of North Anatolian Fault Zone in NW Turkey, has formed the south border of the basin (Yaltırak 2002; Yaltırak and Alpar 2002; Aksoy et al. 2011) (Fig. 1). Two big earthquakes occurred along the Ganos Fault in 1912 (Ambraseys and Jackson, 2000) (Fig. 2). After these two earthquakes, surface faulting, landslides and widespread liquefaction were observed and described along the Gelibolu peninsula and Ganos region by Macovei (1913), Mihailovic (1927) and Ambraseys and Finkel (1987). Aksoy et al. (2011) found that the fault between Gaziköy and Saroz mainly delineated through stream offsets with cumulative slip varying from 10 to 600 m (Fig. 2).

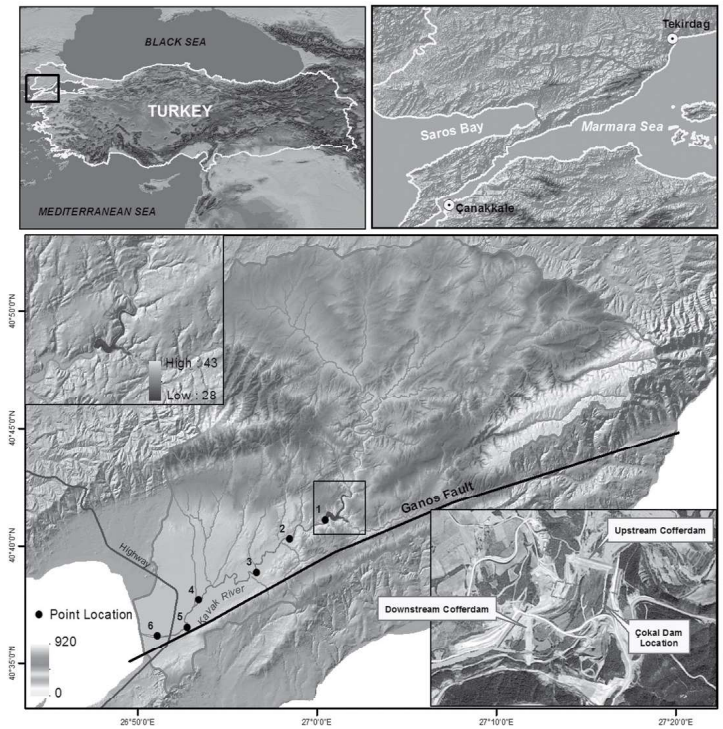


Figure 1: Location map of the study area.

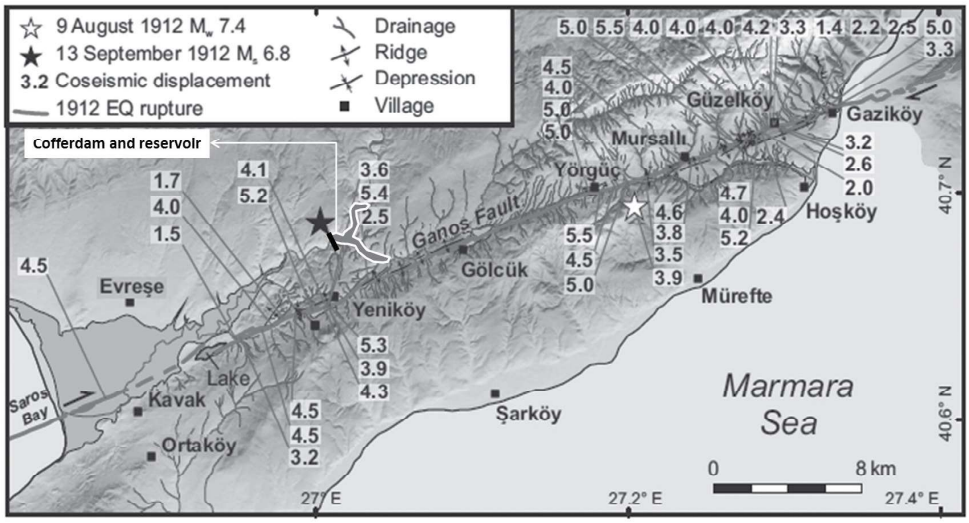


Figure 2: A.D. 1912 coseismic slip distribution (in meters) both white and yellow boxes with the cofferdam location. Modified from Aksoy et al. (2011).

Based on Malkara Meteorological Station (MMS), which is the closest station to the basin, data between 1980 and 2009, a Marmara Transition climate between Black Sea and Mediterranean climates dominates the study area with mean annual rainfall of 683mm received usually during the months of November and December. The November of 2007 has been the wettest month with having 406.4mm total rainfall over the last 30 years (Fig. 3a). Total annual rainfall has been increasing in the last 30 years with increasing variations, especially after the year of 1996 (Fig. 3b). The hottest month is July with an extreme maximum temperature of 40.5°C. February is the coldest month with an extreme minimum temperature of -14.4°C.

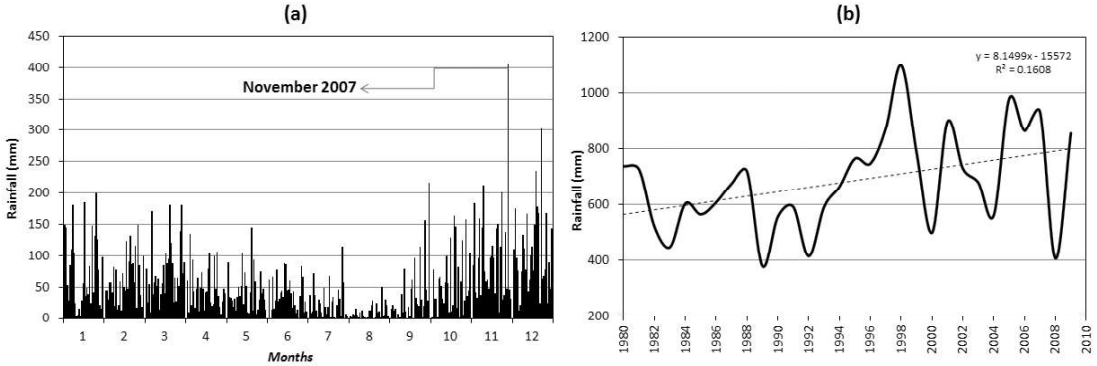


Figure 3: Distribution of (a) total monthly and (b) total annual rainfall data based on MMS between 1980 and 2009.

For the Çokal Dam construction on the Kavak River, two cofferdams, made of earth-fill, were built on the upstream and downstream of the proposed dam location to enable to diversion of the river flow to a tunnel to bypass the dam foundation area. Predominantly flowing from northwest to southeast, Kavak is the main river in the study region. Two branches of the Kavak River in the upstream area collect water from an area of 568 km^2 which also constitutes the upstream cofferdam basin. Below the cofferdams, some tributaries, which drain an area of 205 km^2, join the Kavak River. The upstream and downstream cofferdams were built at 16 m and 3 m height respectively (Fig. 4). The upstream cofferdam failed on the 16th November 2007 due to overtopping as a result of a heavy rainfall event in the region. The water started to overtop at ~13:00, breached the upstream cofferdam at ~14:00 and completely damaged it after ~3-4 hours (Fig. 4). Based on personal communication with the local people, flood water reached the town of Kavak, which is 15 km from the cofferdam, at between 16:00-17:00 and started to fill the upstream side of the Çanakkale-Istanbul highway. At ~01-02am on the 17th November 2007 the water started to drain from the land. Fortunately, no one was killed during this flood event, but most of agricultural areas and farm houses on the Kavak Plain were damaged. After the event, the upstream cofferdam was rebuilt with increased height (Fig. 4).

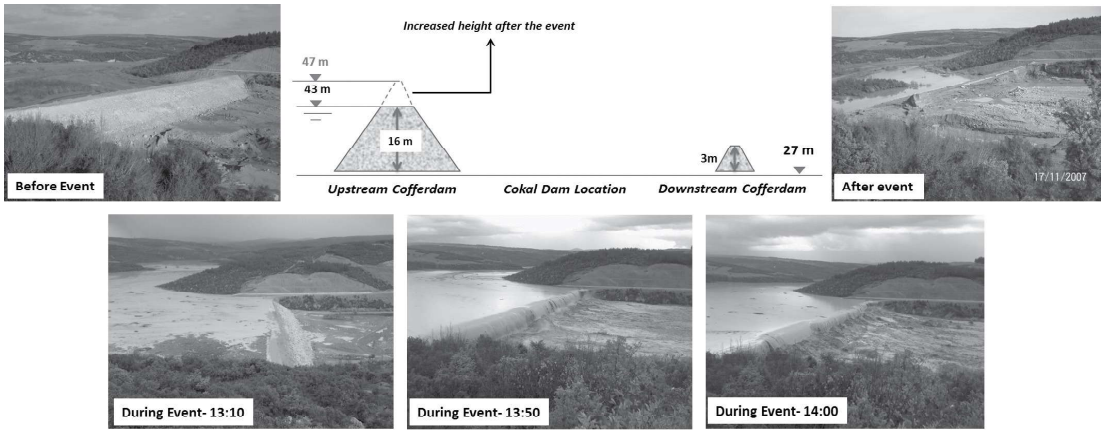


Figure 4: Schematic representation of cofferdams and situation of upstream cofferdam before, during and after event.

Data and Methods

The effect of spatial resolution and impact of altimetric data source on raster-based flood inundation modelling are now well understood according to various applications and testing (e.g. Werner 2001; Horritt and Bates 2001; Wilson and Atkinson 2003a; Wilson and Atkinson 2003b; Wilson and Atkinson 2005;

Casas et al. 2006; Fewtrell et al. 2011; Sampson et al. submitted). The researches show that acquiring topographic map based digital elevation models (DEM) have a low cost; however the accuracy and representation capacity of lowland areas are reduced compared to laser-based data (i.e. Light Detection And Ranging). Laser-based models are expensive, but economically viable for large areas and provide very precise results with decreasing errors. In addition, a high-resolution model gathered from LiDAR is advantageous when small scale processes have significant effect on the model prediction, for example, where inundation extent is controlled by small topographic features such as dykes, levees and ditches (Horritt and Bates 2001). However, the acquisition of this type of data is not easy or common in many countries due to restrictions and costs. As a result, incorporation of surveyed points to the topographic map based models is generally used to enable improved model accuracy. Casas et al. (2006) found that incorporation of bathymetry and GPS points with contours (5 m interval) gives more accurate results, more like LiDAR data in hydraulic modelling. In this study, contour vectors gathered 1:25000 scaled topographic maps were used incorporating GPS points and some measurements on the river channel. GPS points were taken along the Çanakkale-Istanbul highway, which passes the Kavak Plain in a roughly south-north direction, and in the river channel and were added to DEM data (Fig. 5). Therefore, the representational capacity of DEM used in the breach inundation modelling was increased.

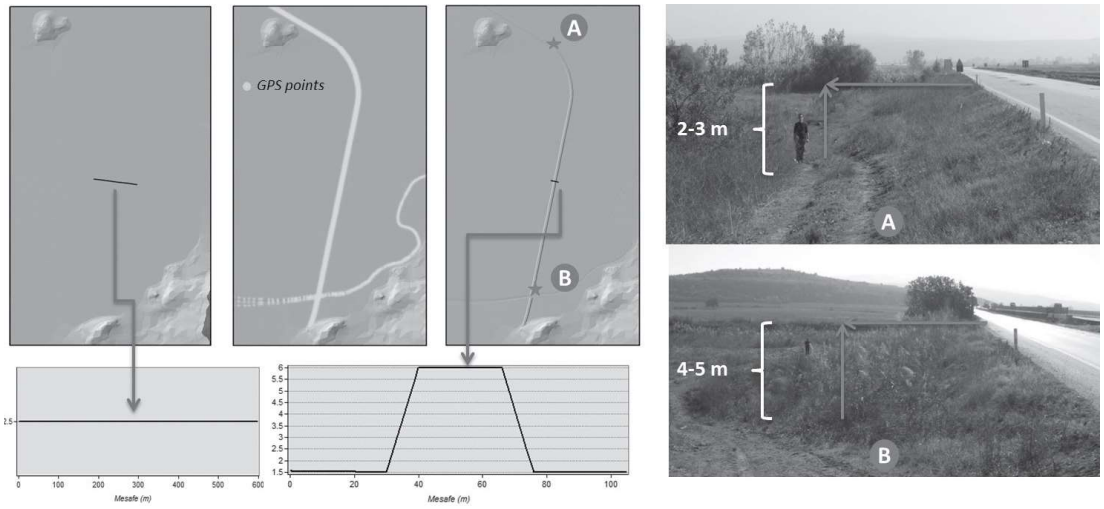


Figure 5. Modifying DEM data using GPS points and field measurements.

As the LISFLOOD-FP model codes have not yet physically suitable for hydraulic jump (Neal et al. in press), breach hydrograph of the upstream cofferdam was established outside of the model depend largely on reservoir storage volume and reservoir water depth above the final breach bottom. In this study, based on 10m DEM data, ~12.307.513 m^3 was used as the volume of the reservoir above the final breach bottom (V_w) and 16m as the difference in elevation between the initial water surface elevation and base elevation of breach (h_w). Based on parameter richness, regression equations following McDonald and Langridge-Monopolis (1984), Froehlich (1995 a,b) and Chinnarasri et al. (2004) were applied to predict peak discharge (Q_p) and failure time (t_f) of breach in order to create an outflow hydrograph (Table 1). MacDonald and Langridge-Monopolise (1984) utilized 42 data sets (earth-fill, earth-fill with a clay core and rock-fill) to develop a relationship for the breach formation factor defined as the product of the volume of breach outflow and depth of water above the breach invert at the time of failure. They found a best fit analysis and boundary curves on 42 failed earth dams in order to determine peak outflow. They also estimated the quantity of eroded embankment materials V_{er} (m^3) for earth dams based on time of failure (t_f). Froehlich (1995 a, b) utilized 22 and 63 data sets which are earthen, earthen with a core wall (i.e. clay) and rock-fill to develop a set of equations to estimate peak breach flow, breach width, side slope and failure time. Chinnarasri et al. (2004) proposed and expressed a set of equations combining of experimental results and historical dam failure data to represent the possible maximum peak outflow and possible minimum peak outflow from the breach; they also presented the relation between the breach deformation time and the reservoir shape characteristic and the peak outflow. They found that the predicted values using the proposed equations yield closer to results than the others. Using the equations given in Table 1, three different breach outflow hydrographs were produced based on triangular unit hydrograph methods (NEDC 1999). It is assumed that time to peak (T_p) occurred at the end of the failure time (t_f) and the receding limb time of the hydrograph is equal to 1.67 T_p.

Table 1: Regression equations used to estimate peak flow and failure time of breach.

References	Peak Flow ($m^3 s^{-1}$)	Failure time
MacDonald and Langridge-Monopolise (1984) $Q_p = m^3 s^{-1}$ $t_f = hour$	$Q_p = 1.154\ (V_w h_w)^{0.412}$	$t_f = 0.0179\ (V_{er})^{0.364}$ $V_{er} = 0.0261\ (V_w h_w)^{0.769}$
Froehlich (1995 a, b) $Q_p = m^3 s^{-1}$ $t_f = hour$	$Q_p = 0.607\ (V_w^{0.295} h_w^{1.24})$	$t_f = 0.00254\ (V_w)^{0.53}\ h_w^{-0.9}$
Chinnarasri et al. (2004) $Q_p = m^3 s^{-1}$ $t_f = second$	$Q_{pmax} = 0.66\ (V_w^{0.30} h_w^{1.61})$ $Q_{pmin} = 0.06\ (V_w^{0.26} h_w^{1.71})$	$t_f = 5.84\ V_w^{0.75}\ h_w^{0.76} Q_p^{-1}$

LISFLOOD-FP model is used here as there are a number solution schemes of varying complexity implemented within the same numerical code. All models utilise the same input files and data structures, along with many shared subroutines. In fact, as the continuity equations are the same for all models, they only differ in respect of the flow equations and time stepping. The numerical schemes used in this study (Inertial LISFLOOD-FP and LISFLOOD-Roe) are described as below.

Inertial formulation of the two dimensional shallow water equations was developed by Bates et al. (2010) due to the computational cost of the diffusive form of the St. Venant equations. The model which is designed to be solved explicitly at very low computational cost was incorporated into the LISFLOOD-FP model code where flow between neighbouring floodplain cells is calculated as in Eq. 1:

$$q^{t+\Delta t} = \frac{q^t - gh_{flow}^t \Delta t \frac{\Delta(h^t+z)}{\Delta x}}{\left(1+gh_{flow}^t \Delta t n^2 |q^t| / \left(h_{flow}^t\right)^{10/3}\right)} \quad (1)$$

where q is the flow per unit width [L^2T^{-1}], g is the acceleration due to gravity [LT^{-2}], h_{flow} is the depth of water available to flow [L] and Δt is the model time step [T], Δx is the model grid resolution [L], z is the bed elevation [L], h is the water depth [L] and n is the Manning's friction coefficient [$L^{-1/3}T$]. Water depths are consequently updated using the finite difference discretised form of the continuity equation using discharge between cells, Q [L^3T^{-1}], as in Eq. 2:

$$h_{i,j}^{t+\Delta t} = h_{i,j}^t + \Delta t \frac{Q_{x\,i-1,j}^t - Q_{x\,i,j}^t + Q_{y\,i,j-1}^t - Q_{y\,i,j}^t}{\Delta x^2} \quad (2)$$

The stability is controlled by the Courant-Freidrichs-Levy (CFL) conditions for shallow water flows such that the stable model time step, Δt, is a function of the grid resolution, Δx, and the maximum water depth, h, within the domain (Bates et al. 2010):

$$\Delta t_{max} = \propto \frac{\Delta x}{\sqrt{gh_t}} \quad (3)$$

where α is a coefficient in the range between 0.2 and 0.7 used to produce a stable simulation.

LISFLOOD-Roe is the two-dimensional shallow water model and it calculates the flow according to the complete Saint Venant formulation (Villanueva and Wright 2006). The method is based on the Godunov approach and uses an approximate Riemann solver by Roe (Roe 1981). It solves the full shallow water equations with a shock capturing scheme. LISFLOOD-Roe uses a point-wise friction based on the Manning´s equation, while the domain boundary/internal boundary (wall) uses the ghost cell approach. The stability of this approach is approximated by the

CFL condition for shallow water models. As the complete model formulation is quite lengthy and relatively well known it is not given here.
Produced DEM and hydrographs were used and tested in the Inertial and Roe numerical codes implemented to LISFLOOD-FP to enable the modelling of the flood following the cofferdam breaching in the Kavak floodplain. Friction was represented as one single composite value of n=0.050. This was selected based on the spatial distribution of land use type (mostly agricultural land) within the domain as determined from high resolution satellite images. Based on real flood event in the area, total simulation time was set up 16 hours with 30 minutes saving intervals. The maximum flood extents based on different hydrographs and numerical models were compared with the real flood extent, mapped by Ozdemir et al. (2011) from one day after the event fieldwork data and personal communication with local people, using the following fit statistic (Aronica et al. 2002; Horritt and Bates 2002):

$$F = \frac{Num(S_{mod} \cap S_{obs})}{Num\,(S_{mod} \cup S_{obs})} x\ 100 \qquad (4)$$

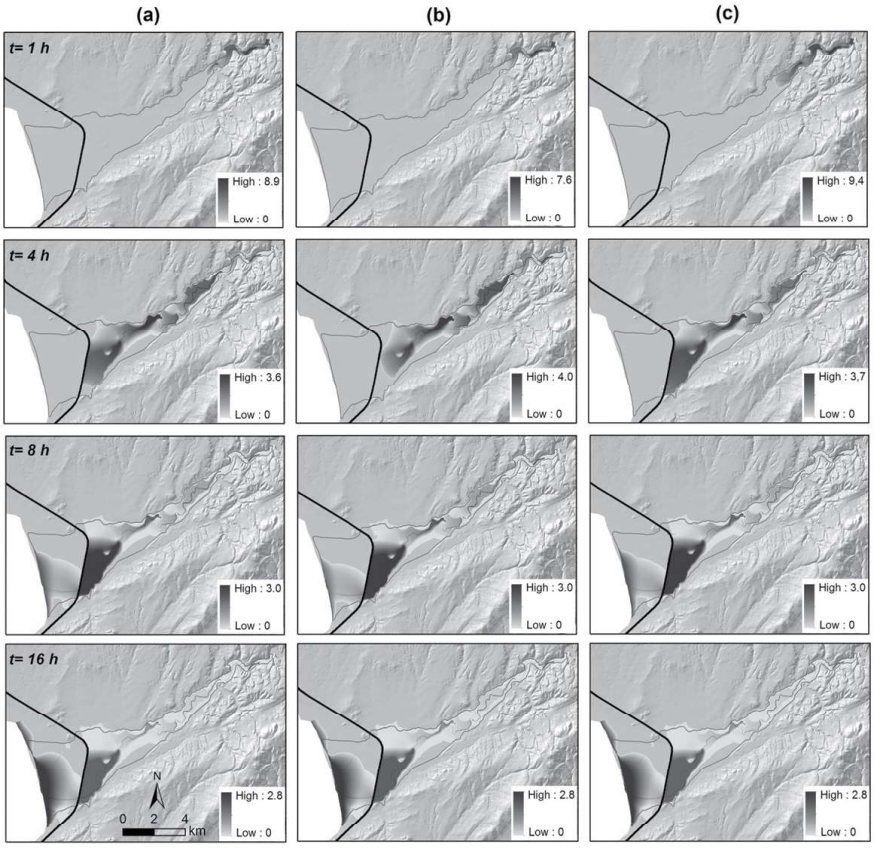
S_{mod} and S_{obs} are the sets of domain sub-regions (pixels, elements or cells) predicted as flooded by the model and observed to be flooded, and Num(.) denotes the number of members of the set. F therefore varies between 0 for model with no overlap between predicted and observed inundated areas and 100 for a model where coincide perfectly. This measure allows a useful comparison between model performance for different modelled reaches and flood events.

Results and discussion

Applying the MacDonald and Langridge-Monopolis (1984), Froehlich (1995 a,b) and Chinnarasri et al. (2004) equations, given in Table 1, to the upstream cofferdam of Cokal Dam failure with a reservoir volume at the time of failure of 12.307.513 m^3 and a height of water of 16 m, provides a peak flow estimate of 3016.15 m^3s^{-1}, 2332.91 m^3s^{-1} and 4078.5 m^3s^{-1} (mean peak outflow based on maximum and minimum peak outflow equations of Chinnarasri et al. 2004) respectively. In the same chronological order, applying failure time equations given Table 1, gives 1.00 h, 1.20 h and 0.68 h, and total hydrographs end 2.67 h, 3.20 h and 1.82 h respectively, using triangular unit hydrograph formulae. Using the produced peak outflows and unit hydrographs, the Inertial and Roe models were constructed at modified Δx=10m resolution DEM. Figure 6 and 7 show the propagation of the flood wave at four times (1, 4, 8 and 16 hours). The flood water enters the domain at the upstream cofferdam location and flows down the southwest direction into the Kavak Plain. After flowing ~15 km, the water

reaches to Çanakkale-Istanbul highway in around 4 hours according to both the inertial and Roe models. After 4 hours, the water starts to collect behind the Çanakkale-Istanbul highway worked second dam but can only pass through at the Kavak Bridge location and a small culvert in the north. All the simulations were ended after 16 hours, based on the real flood event duration. As the flood wave propagates through the Kavak Plain, there are some differences in simulated water depth between the inertial and Roe model. These differences are not bigger than 0.5m at the four time steps given in Figure 6 and 7. Maximum water depth is greater by ~5% in the Roe model than the inertial model.

Figure 6: Progression of flooding predicted by the inertial model with using breach formulas (a) MacDonald and Langridge-Monopolis (1984), (b) Froehlich (1995a,b), (c) Chinnarasri et al (2004). Red outline and black line represent observed flood extent and Çanakkale-Istanbul highway respectively



Between the breach formulas in the both models, the maximum water depth differences are ~8%. The breach inundation model based on the Chinnarasri et al. (2004) formula has maximum water depths of 9.8m for the inertial model and

10.4m for the Roe models. Flood water reaches these depths at the beginning of the cofferdam breach and, when the cofferdam height during the breach is taken into consideration (Fig. 4), the depth values are quite acceptable.

The effects of the hydrographs and the models were investigated also by comparing inundation areas and volumes over time. Figure 8 shows the inundation areas and volumes over time for all breach flow predictions in both models. Based on the breach flow hydrograph, the inundation area and volume calculated according to Chinnarasri et al. (2004) are higher during the inflow domain in the both models. However, after the inflow, the inundation area and the volume of the MacDonald and Langridge-Monopolis (1984) prediction is larger.

Figure 7: Progression of flooding predicted by the Roe model with using breach formulas (a) MacDonald and Langridge-Monopolis (1984), (b) Froehlich (1995a,b), (c) Chinnarasri et al (2004). Red outline and black line represent observed flood extent and Çanakkale-Istanbul highway respectively.

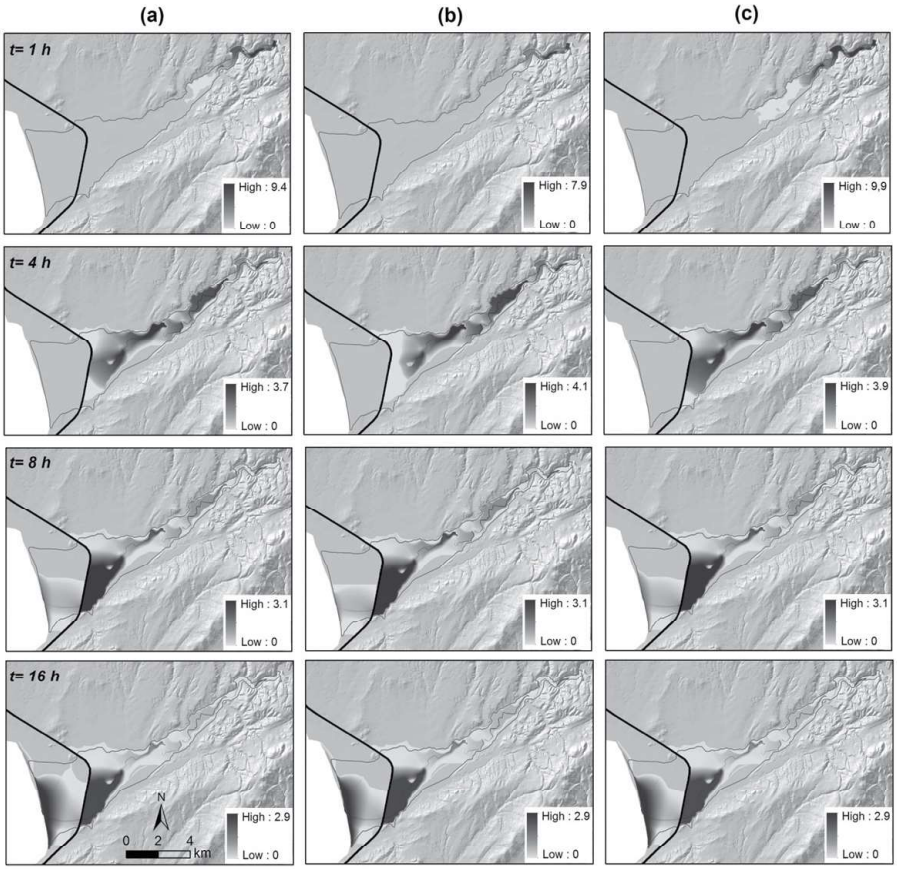
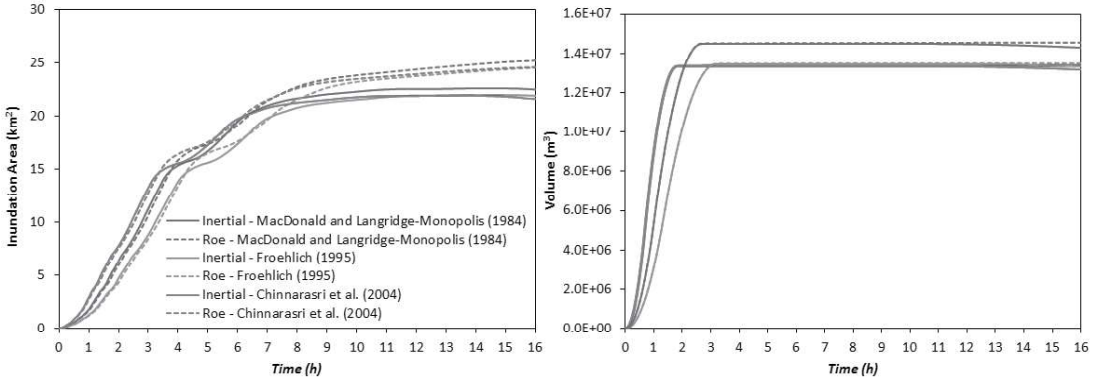


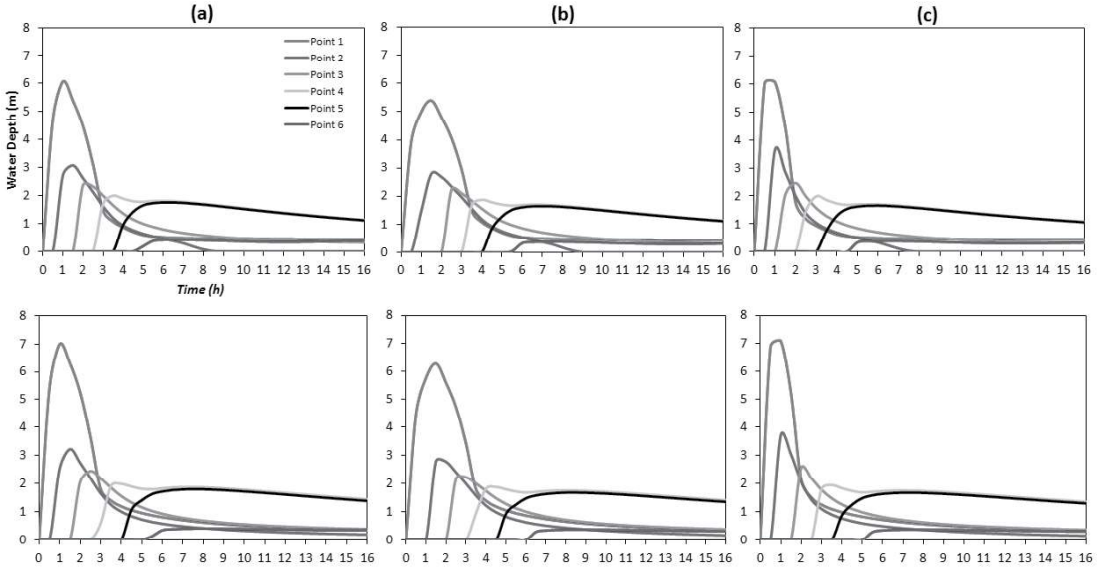
Figure 8: Inundation area and volume versus time with different breach flow prediction formulas and the models.



As a maximum inundation area, the Roe model simulated a greater inundation extent than the inertial model with variations of between 2% - 6%. However, the mass errors (difference between the net inflow through the boundaries and the change in the water volume inside the domain, integrated over time shows the numerical precision of the continuity equation) for Roe model ($-1.2x10^{-3}$) were significantly higher than the inertial model ($-1.9x10^{-7}$) in this case.

Figure 9: shows the evolution of water depths and arrival times of water at 6 control points (see Fig.1). Point 1 represents an area of water depth that is relatively much higher due to its proximity to the cofferdam; points 2 and 3 represent equal distance locations (~4 km) from the point 1. Point 4 represents an area where a small bridge is located on the Kavak River, point 5 is located in the Kavak town and point 6 characterizes an area after Çanakkale-Istanbul highway. All the points' locations were taken on overbank the Kavak River. The water depth differences at point 1 to differ between formulas and models, reaching a variation of ~15% between the models. The difference in arrival times at point locations depends on inflow durations, Q_p values and the model type. For instance, in Chinnarasri et al. (2004) formula, the inflow ends in 1.82 h with 4078.5 m^3s^{-1} of Q_p and the water reaches point 6 in 4.5 hours and 5 hours in the inertial and Roe model respectively. However, based on the real flood event information about the arrival time of the flood water to Kavak town (4 hours), only the Froehlich (1995 a,b) prediction in the inertial model and the MacDonald and Langridge-Monopolis (1984) prediction in the Roe model are accurate at point 5.

Figure 9: Profiles of simulated water depth through time at the six control points using (a) MacDonald and Langridge-Monopolis (1984), (b) Froehlich (1995 a,b) and (c) Chinnarasri et al. (2004) breach formulas. The inertial model was used on top row plots; the Roe model was used on bottom row plots.



All the breach prediction results in both models were assessed against a real flood map produced after the event by using fit statistic (Eq. 4) set out in Table 2. According to the results, best fit prediction is given by the MacDonald and Langridge-Monopolis (1984) breach flow prediction formula, using the Roe model. This prediction formula also has better fit in the inertial model compared to the others. The Froehlich (1995 a,b) prediction formula has the lowest fit value in this case. The LISFLOOD-Roe model simulated later arrival times with slower increases in water level, greater inundation extent and higher mass errors at 10m resolution DEM than the LISFLOOD-Inertial model (Neal et al. in press). With regard to the parameters of inundation area, arrival time and fit statistic, MacDonald and Langridge-Monopolis (1984) using the LISFLOOD-Roe model gives the best result in the study.

Table 2: Table showing Fit statistic values between the real flood event and the simulations undertaken different breach prediction formulas using the inertial and Roe models.

Breach Flow Formulas	LISFLOOD-Inertial	LISFLOOD-Roe
MacDonald and Langridge-Monopolis (1984)	76.6	79.8
Froehlich (1995 a,b)	75.0	75.4
Chinnarasri et al. (2004)	75.8	75.6

Standard, readily available, and two-dimensional hydraulic models within the LISFLOOD-FP code and breach flow prediction techniques have been assessed with respect to the Cofferdam of Cokal Dam breaching inundation in 2007. This analysis was performed to assess the ability of the LISFLOOD-FP models (inertial and Roe) in breach inundation modelling using a real breaching event. Actually, these types of simpler models were unable to simulate hydraulic jumps and wake zones (Néelz and Pender 2010; Neal et al. in press), as expected, but in this case only inundation models below the cofferdam and the flow propagation on the Kavak Plain were modelled using different boundary conditions based on three breach flow predictions. Such predictions and models are commonly applied to hazard classification and emergency action plans. In particular, the Cokal Dam is located on the active Ganos Fault system where two big earthquakes occurred 100 years ago, and is clearly susceptible to earthquake and related hazards (Aksoy et al. 2011). Predictions and modelling processes for probable breaching must therefore be carried out for the Cokal Dam which has already been constructed (Ozdemir et al. 2011). The Manning's n selection is another important parameter and a uniform Manning's *n* of 0.050 was used in the study due to becoming a representative composite value based on the range of surface roughness values found at this study area and extracting the capacity of breach flow predictions and the hydraulic models rather than surface friction variations. As a result, Manning's n values were not calibrated in the models. Breach flow predictions were developed using three regression equation-based methods. The prediction accuracies were found, albeit small, underestimate (the best one is 79.8%) with the mapped real flood extent of the Cofferdam failure. Increasing the DEM resolution especially on the Kavak Plain and adding the discharge of tributaries join the Kavak River after the dam site (Ozdemir et al. 2011) might increase the models and prediction accuracy and further work can be focused on these.

Conclusions

On November 16, 2007 the Cofferdam of Cokal Dam failed due to high intensity rainfall in the region. ~12 million cubic meter water were released from the upstream cofferdam and all the agricultural areas on the Kavak Plain were inundated. A LISFLOOD-FP hydraulic model was constructed of the failure to assess the capability of the inertial and Roe models, using different breach hydrographs to predict the movement of the cofferdam breach flood wave downstream at 10m resolution DEM. The MacDonald and Langridge-Monopolis (1984) breach flow prediction gave the best results in both the LISFLOOD-FP

models with 3016.15 m^3s^{-1} of peak flow and total 2.67 hours inflow compared to the Forehlich (1995 a,b) and Chinnarasri et al. (2004). The Roe model gave the better results in terms of inundation area, arrival times and fit statistic although it has higher mass errors than the inertial model.

The results of hydraulic modelling depend mainly on the DEM quality and representation capacity of the surface. In this study, adding of Çanakkale-Istanbul highway platform data to topographic contour intervals using GPS points and field measurements increased the representation capacity of the Kavak Plain in the 10m resolution DEM (Casas et al. 2006). In all models the highway platform worked like a second dam and retained the flood water behind it, as in the real event. Therefore, this platform must be reconstructed with more culverts to cope with probable future floods. Finally, because of the hazard susceptibility of the study area, future work should concentrate on probable dam breach inundation modelling using two-dimensional hydraulic models, high resolution DEM, and considering the discharge of the tributaries joining the Kavak River below the Dam site.

Acknowledgements

This work was supported by the Research Fund of the Istanbul University with Project No: 4400 and by TUBITAK (The Scientific and Technological Research Council of Turkey) with program of 2219. The author would like to thanks to Mr. Dogan UNERI and Mr. Dick WILLIS for their helps.

References

Ambraseys NN, Finkel CF (1987) The Saros- Marmara earthquake of 9 August 1912. Earthquake Engineering & Structural Dynamics Vol 15:189–211.

Ambraseys NN, Jackson JA (2000) Seismicity of the Sea of Marmara (Turkey) since 1500. Geophysical Journal International V 141 No 3:F1–F6.

Aksoy ME, Meghraoui M, Vallee M, Cakır Z, (2010) Rupture characteristics of the A.D. 1912 Murefte (Ganos) earthquake segment of the North Anatolian fault (western Turkey). GSA Geology V 38 no 11:991-994.

Aronica G, Bates PD, Horritt MS (2002) Assessing the uncertainty in distributed model predictions using observed binary pattern information within GLUE. Hydrological Processes 16:2001–2016.

Bates PD, De Roo APJ (2000) A simple raster-based model for flood inundation simulation. Journal of Hydrology 236 (1-2):54-77.

Bates PD, Horritt MS, Fewtrell TJ, (2010) A simple inertial formulation of the shallow water equations for

efficient two dimensional flood inundation modelling. Journal of Hydrology 387(1-2):33-45.

BSHM (Big Sky Hazard Management) (2004) Silver Bow County Hazard Mitigation Plan. February 2004.

Casas A, Benito G, Thorndycraft VR, Rico M, (2006) The topographic data source of digital terrain models as a key element in the accuracy of hydraulic flood modelling. Earth Surface Processes and Landforms 31: 444-456.

Chang TJ, Hsu MH, Teng WS, Huang CJ, (2000) A GIS-assisted distributed watershed model for simulating flooding and inundation. J Am Water Resour Assoc 36 (5):975–988.

Chen AS, Hsu MH, Chen TS, Chang TJ (2005) An integrated inundation model for highly developed urban areas. Water Sci Technol 51 (2): 221–229.

Chinnarasri C, Jirakitlerd S, Wongwises S (2004) Embankment dam breach and its outflow characteristics. Civil Engineering and Environmental Systems Vol 21 No. 4:247-264.

Costa JE (1985) Floods from Dam Failures. US Geological Survey Open-File Report 85–560. Denver Colorado 54.

De Maio A, Savi F, Sclafani L (2004) Three-dimensional mathematical simulation of dambreak flow. Proceeding of IASTED conferences–Environmental Modelling and Simulation St Thomas US Virgin Island, ISBN 0-88986-441-1.

EM-DAT (2011) The OFDA/CRED International Disaster Database – www.emdat.be, Université Catholique de Louvain, Brussels (Belgium).

Evans SG (1986) The Maximum Discharge of Outburst Floods Caused by the Breaching of Manmade and Natural Dams. Canadian Geotechnical Journal 23(3): 385–387.

Fewtrell TJ, Duncan A, Sampson CC, Neal JC, Bates PD (2011) Benchmarking urban flood models of varying complexity and scale using high resolution terrestrial LiDAR data. Physics and Chemistry of the Earth 36:281-291.

Fread DL (1988) BREACH An erosion model for earthen dam failures. National Weather Service (NWS) NOAA Silver Spring Maryland USA.

Fread DL (2000) NWS FLDWAV Model: Theoretical Description. Hydrologic Research Laboratory Office of Hydrology National Weather Service NOAA March 6 2000.

Froehlich DC (1995a) Embankment Dam Breach Parameters Revisited. Proceedings of the 1995 ASCE Conference on Water Resources Engineering San Antonio Texas August: 887-891.

Froehlich DC (1995b) Peak Outflow from Breached Embankment Dam. Journal of Water Resources Planning and Management Vol 121 No 1:90-97.

Froehlich DC (2008) Embankment dam breach parameters and their uncertainties. Journal of Hydraulic Engineering Vol 134 No 12:1708–1721.

Hagen VK (1982) Re-evaluation of Design Floods and Dam Safety. Proceedings of the 14th International Commission on Large Dams Conference Rio de Janeiro Brazil.

Hydrologic Engineering Center (HEC) (2010) HEC-RAS River Analysis System User's Manual Ver

4.1. U.S. Army Corps of Engineers Davis, CA.

Horritt MS, Bates PD (2001) Effects of spatial resolution on a raster based model of flood flow. Journal of Hydrology 253: 239–249.

Hsu MH, Chen SH, Chang TJ (2000) Inundation simulation for urban drainage basin with storm sewer system. Journal of Hydrology 234:21–37.

Hunter NM, Horritt MS, Bates PD, Wilson MD, Werner MGF (2005) An adaptive time step solution for raster-based storage cell modelling of floodplain inundation. Advances in Water Resources 28(9):975-991.

Kirkpatrich GW (1977) Guidelines for Evaluating Spillways Capacity. Water Power and Dam Construction 29(8):29–33.

McDonald TC, Langridge-Monopolis J (1984) Breaching Characteristics of Dam Failures. Journal of Hydraulic Engineering Vol 110 No 5:567-586.

Macovei G (1913) Aspura Cutremurului de Pamant dela Mare de Marmara dela 9 August 1912. Academia Romana. Publicatiunile Adamachi Vol 33:260–273.

Mihailovic J (1927) Trusne katastrofe na Mramornome moru. *in* Posebno izdanje srpse akademija nauka Volume 65:1–303.

Mohammadi M (2008) Boundary shear stress around bridge piers. Am J Appl Sci 5(11):1546–1550.

Nagata N, Hosoda T, Nakato T, Muramoto Y (2005) Three-dimensional numerical model for flow and bed deformation around river hydraulic. J Hydraul Eng ASCE131:1074–1087.

NEDC (National Employee Development Center) (1999) Module 207 Hydrograph Development. USA.

Néelz S, Pender G (2010) Benchmarking of 2D Hydraulic Modelling Packages. SC080035/SR2. Environment Agency, Bristol.

Neal JC, Villanueva I, Wright N, Willis T, Fewtrell T, Bates PD (in press) How much physical complexity is needed to model flood inundation? Hydrological Processes DOI: 10.1002/hyp.8339.

Ozdemir H, Akbulak C, Ozcan H (2011) Çokal Barajı (Çanakkale) çökme modeli ve taşkın risk analizi. Uluslararası İnsan Bilimler Dergisi Cilt 8 Sayı 2:559-698.

Rico M, Benito G, Diez-Herrero A (2008a) Flood from tailing dam failures. J Hazard Mater 154 (1-3): 79-87.

Rico M, Benito G, Salgueiro AR, Diez-Herrero A (2008b) Reported tailing dam failures: A review of the European incidents in the worldwide context. J Hazard Mater 152(2): 846-852.

Roe P (1981) Approximate Riemann Solvers, Parameter Vectors, and Difference-Schemes. Journal Of Computational Physics 43(2): 357-372.

Sampson CC, Fewtrell TJ, Duncan A, Shaad K, Horritt MS, Bates PD (submitted) Using terrestrial laser scanning data to drive decimetric resolution urban inundation models.

SCS (1981) Simplified Dam-Breach Routing Procedure. Technical Release No 66 (Rev.1) p39.

Singh KP, Snorrason A (1984) Sensitivity of Outflow Peaks and Flood Stages to the Selection of Dam Breach Parameters and Simulation Models. Journal of Hydrology Vol 68:295-310.

Singh VP, Scarlatos PD (1989) Breach erosion model of earthfill dams and flood routing (BEED) model. Miscellaneous Paper EL-79-6 Military Hydrology Report 14. US Army Engineering Waterways Experiment Station Mississippi.

Sümengen M, Terlemez I (1991) Güneybat Trakya yöresi Eosen çökelleri stratigrafisi. MTA Dergisi 113: 17–30.

Tingsanchali T, Chinnarasri C (2001) Numerical modelling of dam failure due to flow overtopping. Hydrological Science Journal 46(1): 113–130.

Toro EF (2001) Shock-capturing methods for free-surface shallow flows. Wiley, Chichester.

Toro EF, Garcia-Navarro P (2007) Godunov-type methods for free-surface shallow flows: A review. J Hydraulic Res 45(6):736–751.

Villanueva I, Wright NG (2006) Linking Riemann and storage cell models for flood prediction. Proceedings of the Institution of Civil Engineers. Journal of Water Management 159:27-33.

Von Thun JL, Gillette DR (1990) Guidance on Breach Parameters. Unpublished Internal Document US Bureau of Reclamation Denver Colorado 17 pp.

Wang Y, Liang Q, Kesserwani G, Hall JW (2011) A 2D shallow flow model for practical dam-break simulations. Journal of Hydraulic Research 49:3:307-316.

Warren AL (2011) Investigation of dam incidents and failures. Forensic Engineering Volume 164 Issue FE1:33-41.

Werner MGF (2001) Impact of grid size in GIS based flood extent mapping using a 1D flow model. Physics and Chemistry of the Earth (B) 26(7–8): 517–522.

Wilson MD, Atkinson PM (2003a) Prediction Uncertainty in Elevation and its Effects on Flood Inundation Modelling. The Seventh International Conference on Geocomputation, Southampton.

Wilson MD, Atkinson PM (2003b) A Comparison of Remotely Sensed Elevation Data Sets for Flood Inundation Modelling. The Seventh International Conference on Geocomputation, Southampton.

Wilson MD, Atkinson PM. (2005) The use of elevation data in flood inudation models: a comparison of ERS In SAR and combined contour and Differential GPS. International Journal of River Basin Management 3(1): 3–30.

Yaltırak C (2002) Tectonic evolution of the Marmara Sea and its surroundings. Mar Geol 190, S0025-32 27(02)00360-2.

Yaltırak C, Alpar B (2002) Kinematics and evolution of the northern branch of the North Anatolian Fault (Ganos Fault) between the Sea of Marmara and the Gulf of Saros. Marine Geology 190:351-366.